Measurement of the WW Production Cross Section in $p\bar{p}$ collisions at $\sqrt{s} = 1.96$ TeV using 3.6 fb^{-1} of CDF Run II Data

The CDF Collaboration
URL http://www-cdf.fnal.gov
(Dated: April 20, 2009)

We report a new measurement of the WW production cross section in the two charged lepton (e,μ) and two neutrino final state in $p\bar{p}$ collisions at a center of mass energy of 1.96 TeV. The data were collected with the CDF II detector at the Tevatron collider at Fermilab and correspond to an integrated luminosity of approximately 3.6 fb^{-1}. Matrix element based likelihood ratios (LR_{WW}) are used to distinguish the WW signal from backgrounds in the final selection region. The WW cross section is then extracted using a binned maximum likelihood method which best fits the LR_{WW} signal and background shapes to the data. The measured WW cross section is 12.1 ± 0.9 (stat.)$^{+1.6}_{-1.4}$ (syst.) pb.

I. INTRODUCTION

The direct production of WW pairs in proton-antiproton collisions is the primary background in searches for a high mass Standard Model Higgs boson decaying to WW. A good understanding and modeling of WW production is thus essential to any Higgs to WW search. Studying WW production at the Tevatron also provides an opportunity to explore $\sqrt{s}$ energies higher than those available at the LEP collider. Both Tevatron experiments have measured the WW production cross section in the past [1, 2], and the DØ experiment has recently released a new preliminary result [3]. This note presents the most precise measurement to date of the WW production cross section in $p\bar{p}$ collisions at $\sqrt{s} = 1.96$ TeV. We use approximately 3.6 fb^{-1} of integrated luminosity collected by the CDF II detector at the Fermilab Tevatron.

The WW production cross section was first measured by CDF in Run II using 184 pb^{-1} of data. This was performed as a counting experiment, and gave the result $\sigma(p\bar{p} \to W^+W^-) = 14.6^{+6.1}_{-6.0}$ with all uncertainties combined [2]. A second measurement was made using 825 pb^{-1} of data, also as a counting experiment, and found $\sigma(p\bar{p} \to W^+W^-) = 13.6^{+3.0}_{-3.0}$ with all uncertainties combined [4].

In this note we present a measurement of $\sigma(p\bar{p} \to WW)$ via the decay chain $W^+W^- \to \ell^+\nu\ell^-\bar{\nu}$, where $\ell^\pm = e, \mu$, or τ with final states e^+e^-, $\mu^+\mu^-$, and $e^\pm\mu^\mp$. We require there be zero reconstructed jets in the final state. In 3.6 fb^{-1} of data, we find 654 events, about half of which are expected to be WW events with the other half coming from Standard Model backgrounds. To measure the WW cross section, we calculate a matrix element probability for each event to be a WW event. We then form a likelihood ratio and, using background templates derived primarily from Monte Carlo samples, fit the likelihood ratio for the normalization of WW events.

II. EVENT SELECTION

This analysis is based on an integrated luminosity of 3.6 fb^{-1} collected with the CDF II detector between March 2002 and August 2008. The data are collected with inclusive high-p_T lepton (electron or muon) triggers. We use the same data sample and lepton selection as the search for a Higgs boson decaying to two W bosons [5], which involves two(three) categories of electrons(muons). A sixth category, based on central tracks that are not fiducial to calorimeters or muon detectors, is used as either an electron or muon in forming WW candidates.

All leptons are required to be isolated such that the sum of the E_T for the calorimeter towers in a cone of $\Delta R = \sqrt{(\Delta\eta)^2 + (\Delta\phi)^2} < 0.4$ around the lepton is less than 10% of the electron E_T or muon p_T. The transverse energy E_T of a shower or calorimeter tower is $E\sin\theta$, where E is the associated energy. Similarly, p_T is the component of track momentum transverse to the beam line.

Electron candidates are required to have a ratio of HAD energy to EM energy consistent with originating from an electromagnetic shower and are further divided into central and forward categories. The central electron category requires a well-measured track satisfying $p_T > 10$ GeV/c that is fiducial to the central shower maximum detector (SMX) and matched to a central EM energy cluster. The candidate is also required to have a matching cluster in the SMX, minimal energy sharing between towers, and a ratio for shower energy E to track momentum p of less than $2.5 + 0.0015E_T$. A forward electron is required to be fiducial to the forward SMX detector and have an energy deposition in both the calorimeter towers and SMX detector consistent with an electron shower shape. One of the calorimeter seeded tracks is required to be matched with a silicon track to reduce the photon background.

Muons are identified by either a charged track matched to a reconstructed track segment ("stub") in muon chambers or as a stubless minimum ionizing particle fiducial to the calorimeters. In addition, stubless muons are required to have at least 0.1 GeV in total calorimeter energy. For $|\eta_\mathrm{det}| < 1.2$, strict requirements on the number of tracking chamber hits and the χ^2 of the track fit are placed on the muon tracks in order to suppress kaon decay-in-flight backgrounds. The category of stubless muons with $|\eta_\mathrm{det}| > 1.2$ requires that at least 60% of the tracking chamber layers crossed by the track have hits. In order to suppress background from cosmic rays, the track's point of closest approach to the beamline must be consistent with originating from the beam line.

The final category of leptons are constructed from tracks which are not fiducial to the SMX detectors nor identified as stubbed muons. The requirements for the tracks are the same as stubless muons with $|\eta_\mathrm{det}| < 1.2$, but without any of the calorimeter requirements. Due to the lack of calorimeter information, electrons and muons cannot be reliably differentiated in this region, and are therefore treated as having either flavor in the candidate selection.

To identify the presence of neutrinos, we use the missing transverse energy $\not{E}_\mathrm{T} = |\sum_i E_{T,i} \, \hat{n}_{T,i}|$, where the $\hat{n}_{T,i}$ is the transverse component of the unit vector pointing from the interaction point to calorimeter tower i. The $\not{E}_\mathrm{T}$ is corrected for muons which do not deposit all of their energy in the calorimeter.

Candidate events are required to pass one of four online trigger selections implemented in three successively more stringent levels. The final central electron requirement is an EM energy cluster with $E_\mathrm{T} > 18$ GeV matched to a track with $p_\mathrm{T} > 8$ GeV/c. Muon triggers are based on information from muon chambers matched to a track with

CDF Run II Preliminary $\int \mathcal{L} = 3.6$ fb^{-1}	
Process	Events
Z/γ^*	79.8 ± 18.4
WZ	13.8 ± 1.9
$W\gamma$	91.7 ± 24.8
W+jets	112.7 ± 31.2
ZZ	20.7 ± 2.8
$t\bar{t}$	1.3 ± 0.2
Total Background	320.1 ± 46.8
WW	317.6 ± 53.8
Signal+Background	637.6 ± 79.4
Data	**654**

TABLE I: Expected signal (WW) and background events for 0-jet events. The integrated luminosity is 3.6 fb^{-1}. Errors shown are systematic uncertainties only.

$p_{\rm T} > 18$ GeV/c. The trigger for forward electrons requires an $E_{\rm T} > 20$ GeV EM energy cluster and an online measurement of the $\not{E}_{\rm T} > 15$ GeV [6].

A. Signal Region

The $\ell\ell\nu\bar{\nu}$ candidates are selected from events with exactly two opposite-sign leptons. At least one lepton is required to satisfy the trigger and have $E_{\rm T} > 20$ GeV ($p_{\rm T} > 20$ GeV/c) for electrons (muons). We loosen this requirement to > 10 GeV (GeV/c) for the second lepton to increase kinematic acceptance. The z-positions of the leptons at the point of closest approach to the beam-line are required to be within 4 cm of each other.

There are several sources of background: Drell-Yan where the measured large $\not{E}_{\rm T}$ is due to resolution tails, $WZ \rightarrow \ell\ell\ell\nu$ where one lepton is lost, $WW \rightarrow \ell\ell\nu\bar{\nu}$, $t\bar{t} \rightarrow b\bar{b}\ell\ell\nu\bar{\nu}$, and $W\gamma$ and W+jets where a photon or jet is misidentified as a lepton.

Jets in the event are required to have $E_{\rm T} > 15$ GeV and $|\eta| < 2.5$. The majority of WW events have zero jets, and as the jet multiplicity increases the backgrounds change (eg. $t\bar{t}$ becomes a larger contribution with increasing jet multiplicity). In this analysis the signal region consists only of events with zero reconstructed jets.

To suppress the Drell-Yan background, we require $\not{E}_{\rm T\,spec} > 25$ GeV for dielectron and dimuon events and $\not{E}_{\rm T\,spec} > 15$ GeV for electron-muon events, where $\not{E}_{\rm T\,spec}$ is defined as:

$$\not{E}_{\rm T\,spec} \equiv \begin{cases} \not{E}_{\rm T} & \text{if } \Delta\phi(\not{E}_{\rm T}, \text{lepton}, \text{jet}) > \frac{\pi}{2} \\ \not{E}_{\rm T} \sin(\Delta\phi(\not{E}_{\rm T}, \text{lepton}, \text{jet})) & \text{if } \Delta\phi(\not{E}_{\rm T}, \text{lepton}, \text{jet}) < \frac{\pi}{2} \end{cases}$$

This definition is a requirement that the $\vec{\not{E}}_{\rm T}$ transverse to each lepton or jet in the event is greater than the minimum threshold if $\vec{\not{E}}_{\rm T}$ points along that object, so that losing energy from just one such object in an event would not allow it to enter the sample. We further require the candidates to have $M_{\ell^+\ell^-} > 16$ GeV in order to suppress heavy flavor contributions.

The expected and observed yields after base selection cuts have been applied are shown in Table I. The WW cross section used to estimate the expected number of WW events was calculated using the MC@NLO program with the new CTEQ6.6 PDFs [7]. The WW cross section calculated by MC@NLO is

$$\sigma_{WW}^{NLO} = 11.66 \pm 0.70 \text{ pb.}$$

III. DATA MODELING

The geometric and kinematic acceptance for the WW, WZ, ZZ, $W\gamma$, Drell-Yan (DY), and $t\bar{t}$ processes are determined using a Monte Carlo calculation of the collision followed by a GEANT3-based simulation of the CDF II detector [8] response. The Monte Carlo generator used for WW is MC@NLO [9]. For WZ, ZZ, DY, and $t\bar{t}$ the generator used is PYTHIA [10], and for $W\gamma$ it is the generator described in [11]. We use the CTEQ5L parton distribution functions (PDFs) to model the momentum distribution of the initial-state partons [12].

A correction of up to 10% per lepton is applied to the simulation based on measurements of the lepton reconstruction and identification efficiencies in data using Z decays. Additional 5% and 10% corrections based on $Z \rightarrow \ell\ell$ cross section

measurements are applied to stubless muons reconstructed from only central tracks and muons reconstructed from minimum ionizing energy deposits in the forward calorimeter, respectively, to account for the known poor modeling of these lepton types. A further correction is applied to the $W\gamma$ background estimate using a measurement of the photon conversion veto efficiency in data. Also, an 8% correction is applied to the WW signal estimate to account for the limited run range of the simulated sample used to estimate the yield. Trigger efficiencies are determined from $W \to e\nu$ data for electrons and from $Z \to \mu^+\mu^-$ data for muons.

The background from W+jets is estimated from a sample of events with an identified lepton and a jet that is required to pass loose isolation requirements and contain a track or energy cluster similar to those required in the lepton identification. The contribution of each event to the total yield is scaled by the probability that the jet is identified as a lepton. This probability is determined from multijet events collected with a set of jet-based triggers. A correction is applied for the small real lepton contribution using single W and Z boson Monte Carlo simulation.

IV. MATRIX ELEMENT AND LIKELIHOOD RATIO FIT

The first step in the measurement of the WW cross section is the formation of an event-by-event matrix element probability density $P_m(x_{obs})$. Four modes (m) are modeled: WW, ZZ, $W\gamma$, and W+jet. The probability density for a given mode m is given by:

$$P_m(x_{obs}) = \frac{1}{<\sigma_m>} \int \frac{d\sigma_m^{th}(y)}{dy} \epsilon(y) G(x_{obs}, y) dy \tag{1}$$

where

x_{obs}	are the observed "leptons" and $\vec{E}_T$,
y	are the true lepton four-vectors (include neutrinos),
σ_m^{th}	is leading-order theoretical calculation of the cross-section for mode m,
$\epsilon(y)$	is total event efficiency $\times$ acceptance
$G(x_{obs}, y)$	is an analytic model of resolution effects, and
$\frac{1}{<\sigma_m>}$	is the normalization.

The function $\epsilon(y)$ describes the probabilities of a parton level object (e, μ, γ, or parton) to be reconstructed as one of the six lepton categories. The efficiency function is determined solely from Monte Carlo for e and μ but comes from a combination of Monte Carlo and data-driven measurements described in Section III for γ and partons. The event probability densities are used to construct a likelihood ratio discriminant:

$$LR_S(x_{obs}) \equiv \frac{P_S(x_{obs})}{P_S(x_{obs}) + \Sigma_i k_i P_i(x_{obs})},$$

where the signal S mode is WW, and k_i is the expected fraction for each background, with $\Sigma_i k_i = 1$.

Because of the missing neutrinos in the final state, the integral in Equation 1 integrates out the unobserved degrees of freedom (DOF) reducing the 12 DOF in y to the eight measured DOF. The likelihood ratio LR_{WW} distribution is shown for each process in Figure 1.

A. Maximum Likelihood Method

A binned maximum likelihood method is used to extract the WW cross section using the shape of the LR_{WW} distributions from signal and background along with their estimated normalizations and systematic uncertainties. The best fit to these distributions, or the maximum likelihood, gives the best measure of the WW cross section.

The likelihood function is formed from a product of Poisson probabilities for each bin in LR_{WW}. Additionally, Gaussian constraints are applied corresponding to each systematic S_c (shown in Table II). The likelihood is given by

$$\mathcal{L} = \left(\prod_i \frac{\mu_i^{n_i} e^{-\mu_i}}{n_i!}\right) \cdot \prod_c e^{\frac{S_c^2}{2}} \tag{2}$$

where μ_i is the total expectation in the i-th bin and n_i is the number of data events in the i-th bin. μ_i is given by

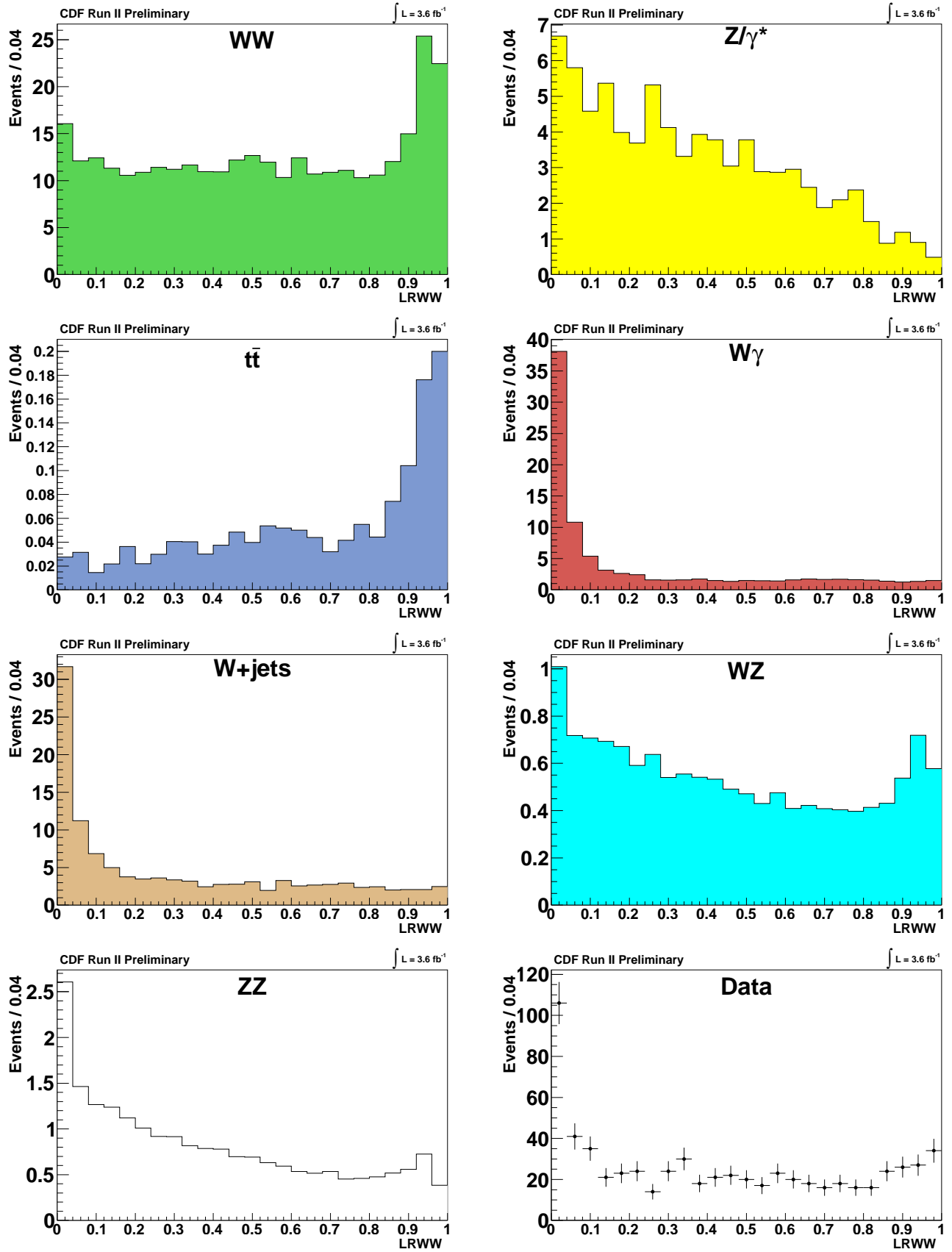$$\mu_i = \sum_k \alpha_k \left[\prod_c (1 + f_k^c S_c)\right] (N_k^{Exp})_i \tag{3}$$

FIG. 1: Likelihood ratio LR_{WW} for each process considered. The integrated luminosity is 3.6 fb^{-1}.

Uncertainty Source	WW	WZ	ZZ	$t\bar{t}$	DY	$W\gamma$	W+jet
Cross Section		6.0%	6.0%	10.0%	5.0%	10.0%	
Acceptance							
PDF Model	1.9%	2.7%	2.7%	2.1%	4.1%	2.2%	
Higher-order Diagrams	5.0%	10.0%	10.0%	10.0%		10.0%	
Jet Modeling	2.0%				21.0%	4.0%	
Conversion Modeling						20.0%	
Jet Fake Rates							27.7%
MC Run Dependence	3.8%			1.0%		5.0%	
Lepton ID Efficiencies	2.0%	1.7%	2.0%	2.0%	1.9%	1.4%	
Trigger Efficiencies	2.1%	2.1%	2.1%	2.0%	3.4%	7.0%	
Luminosity	5.9%	5.9%	5.9%	5.9%	5.9%	5.9%	

TABLE II: Summary of all systematics in this analysis. Systematics in italics are taken to be correlated across processes.

Here f_k^c is the fractional uncertainty associated with the systematic S_c and process k. This is constructed such that the systematics are properly correlated or uncorrelated between the different contributions. $(N_k^{Exp})_i$ is the expected number of events from process k in the i-th bin. α_k is the parameter which is used to measure the WW cross section. It is a freely floating parameter for α_{WW} and fixed to one for all other processes. The measured value of α_{WW} multiplied by the input WW cross section gives the measured value of the WW cross section:

$$\sigma_{WW}^{measured} = \alpha_{WW} \cdot \sigma_{WW}^{NLO}$$

V. SYSTEMATIC UNCERTAINTIES

Systematic uncertainties associated with the Monte Carlo simulation affect the WW, WZ, ZZ, $W\gamma$, DY and $t\bar{t}$ acceptances taken from the simulated event samples. Uncertainties originating from lepton selection and trigger efficiency measurements are propagated through the acceptance calculation, giving uncertainties typically around 2%, but as high as 7%, for the different processes. In the case of the specific muon categories where additional correction factors are applied (see Section III), half of the applied correction is incorporated as an additional uncertainty.

We also assign an acceptance uncertainty due to potential contributions from higher-order effects. In the case of WW we take half of the difference between the leading-order (PYTHIA-based [10]) and next-to-leading order (MC@NLO [9]) acceptances. The background processes are only simulated at leading-order and for these modes we assign the full difference observed in WW, leading to a 10% uncertainty. For the Drell-Yan process, which has been studied extensively at CDF and for which the simulation has been tuned to reproduce the kinematic distributions in data, this uncertainty is small and is included as part of the jet modeling systematic. For Monte Carlo samples not currently generated over the entire data run range, we take additional uncertainties on the acceptance for the corresponding process. This uncertainty is taken from the observed difference in the leading-order WW acceptance for the corresponding partial run range versus that for the full run range. The acceptance variations due to PDF model uncertainties is assessed to be on the order of 2% using the 20 pairs of PDF sets described in [13].

The $E\!\!\!/_T$ resolution modeling uncertainty on the acceptance is determined from comparisons of the data and the Monte Carlo simulation in a sample of dilepton events. For WW, WZ, $ZZ \to \ell\ell\nu\bar{\nu}$, and $t\bar{t}$ production, where one or more neutrinos are responsible for the observed $E\!\!\!/_T$, we determined the uncertainty to be less than 1% and thus negligible. The uncertainty due to the $E\!\!\!/_T$ modeling for the Drell-Yan background is much larger (20%) than for other final states because it depends on the non-Gaussian tails of the resolution function. The $E\!\!\!/_T$ systematic is also included with the jet modeling systematic. The jet modeling systematic accounts for the uncertainty on the modeling of jets in the MC. In the Drell-Yan control region, we see about a 20% difference between the number of events in data with one or more jets, and the number predicted by leading order PYTHIA MC. Because of the much larger number of events with zero jets, 20% uncertainty in the higher jet bins translates to only 5% uncertainty in the zero jet bin. A similar assumption is made for the $W\gamma$ modeling, which also has zero jets at leading order. For the WW, which has zero jets at leading order but is modeled by a next to leading order MC (MC@NLO), the uncertainty is even smaller, at about 2% in the zero jet bin.

For the $W\gamma$ background contribution, there is an additional uncertainty of 20% from the detector material description and conversion veto efficiency. The systematic uncertainty on the W+jets background contribution is determined from differences in the measured probability that a jet is identified as a lepton for jets collected using different jet
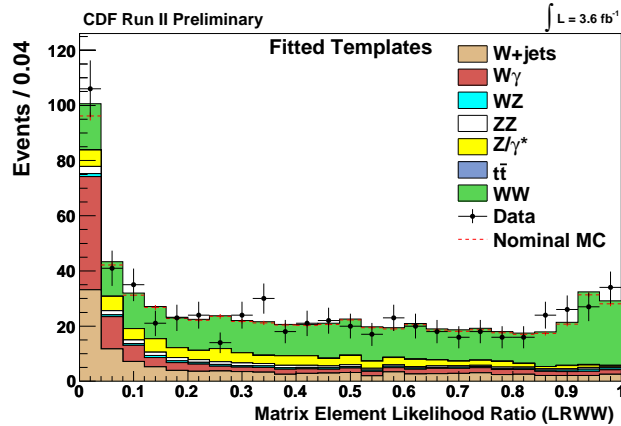
FIG. 2: Fitted signal and background templates where the backgrounds are Gaussianly constrained within their estimated uncertainties and the WW normalization is allowed to float freely. The data is shown as the solid points. Additionally the sum of nominal predictions (before fitting) for all processes is shown as the orange line superimposed.

$E_{\rm T}$ trigger thresholds. These variations correspond to changing the parton composition of the jets and the relative amount of contamination from real leptons.

The uncertainties on the WZ/ZZ, $W\gamma$ and $t\bar{t}$ cross sections are assigned to be 6%, 10% [11], and 10% respectively, where the WZ/ZZ and $t\bar{t}$ cross section uncertainties are based on new theoretical calculations from the Tevatron New Phenomena and Higgs Working Group [14]. In addition, all signal and background estimates obtained from simulation have an additional 5.9% uncertainty originating from the luminosity measurement [15].

The complete set of systematic uncertainties are summarized in Table II.

VI.   RESULTS

The binned maximum likelihood fit to data gives a measured value for the WW cross section of

$$\sigma(p\bar{p} \to WW) = 12.1^{+1.8}_{-1.6} \text{ (pb)} \tag{4}$$

where the uncertainty includes statistical, systematic, and luminosity uncertainties. This corresponds to $\alpha_{WW} = 1.03^{+0.16}_{-0.14}$. Of the Gaussianly constrained systematic uncertainties, none deviates by more than 0.5σ. The fitted templates are shown in Figure 2. Separating out statistical and systematic uncertainties yields

$$\sigma(p\bar{p} \to WW) = 12.1 \pm 0.9 \text{ (stat.) } ^{+1.6}_{-1.4} \text{ (syst.) (pb)} \tag{5}$$

where the systematic uncertainty quoted includes a 5.9% luminosity uncertainty. This is in good agreement with the theoretical expectation of $\sigma(p\bar{p} \to WW) = 11.66 \pm 0.70$ pb, and is the world's best measurement to date of $\sigma(p\bar{p} \to WW)$.

Acknowledgments

---

[1] V. Abazov and *et al.*, Phys. Rev. Lett. **94**, 151801 (2005), see erratum [**?**]., arXiv:hep-ex/0410066v1.

[2] D. Acosta and *et al.*, Phys. Rev. Lett. **94**, 211801 (2005), arXiv:hep-ex/0501050.

[3] V. Abazov and *et al.*, Submitted to Phys. Rev. Lett. (2009), arXiv:0904.0673v1 [hep-ex].

[4] CDF collaboration, *Measurement of the w^+w^- production cross section in 825 pb^{-1} of $p\bar{p}$ collisions at $\sqrt{s} = 1.96$ tev using dilepton events* (2006), see http://www-cdf.fnal.gov/physics/ewk/2006/ww/.

[5] CDF collaboration, *Search for h → ww production using 3.6 fb^{-1}* (2009), see http://www-cdf.fnal.gov/physics/new/hdg/results/hwwmenn_090227.

[6] K. Hagiwara, S. Ishihara, R. Szalapski, and D. Zeppenfeld, Phys. Rev. D **48**, 2182 (1993).

[7] P. Nadolsky and *et al.*, Phys. Rev. D **78**, 013004 (2008), arXiv:0802.0007 [hep-ph].

[8] R. Brun, R. Hagelberg, M. Hansroul, and J. Lassalle, CERN-DD-78-2-REV and CERN-DD-78-2.

[9] S. Frixione and B. R. Webber, JHEP **06**, 029 (2002), hep-ph/0204244.

[10] T. Sjostrand, S. Mrenna, and P. Skands, JHEP **05**, 026 (2006).

[11] U. Baur and E. L. Berger, Phys. Rev. **D47**, 4889 (1993).

[12] H. L. Lai *et al.* (CTEQ), Eur. Phys. J. **C12**, 375 (2000).

[13] S. Kretzer, H. L. Lai, F. I. Olness, and W. K. Tung, Phys. Rev. **D69**, 114005 (2004).

[14] CDF and D0 collaborations, see http://tevnphwg.fnal.gov/.

[15] D. Acosta *et al.*, Nucl. Instrum. Meth. **A494**, 57 (2002).